MATHEMATICAL MODELING AND COMPUTING, Vol. 11, No. 3, pp. 904–910 (2024)

Modeling the thermoelectric characteristics of nanostructured material

Voznyak O. M.[1], Kostrobij P. P.[2], Polovyi B. Ye.[2]

[1] *Vasyl Stefanyk Precarpathian National University, 57 Shevchenko Str., 76018, Ivano-Frankivsk, Ukraine*
[2] *Lviv Polytechnic National University, 12 S. Bandera Str., 79013, Lviv, Ukraine*

(Received 9 May 2024; Revised 25 September 2024; Accepted 27 September 2024)

One-dimensional model of a nanostructured thermoelectric material is considered in case, when the modeled by a potential well nanograin and grain boundaries are represented by potential barriers. The well and barriers are modeled by Gaussian-type potentials. There is developed a software product to calculate the transmission coefficient through the quantum structure "barrier–well–barrier" using the Thomas algorithm. Numerical calculations of the specific conductivity and the Seebeck coefficient for the proposed model are carried out. The calculation results validate the experimental data.

Keywords: *quantum tunneling mechanism of thermoelectric phenomena; model of nanostructured material; Seebeck coefficient; power factor.*

2010 MSC: 65D30, 81V65, 82D80 **DOI:** 10.23939/mmc2024.03.904

1. Introduction

Role of the tunneling mechanism in thermoelectric phenomena became understood as a result of [1–5]. Several studies studied the influence of "energy filtering" of carriers [6] on the thermoelectric coefficient. Developed theory of quantum tunneling mechanism of thermoelectric phenomena for several quantum systems is based on super-lattices with quantum wells, quantum dots, and other thermo-tunneling objects.

On the other hand, there exists a technology based on refining the initial thermoelectric material to sizes of $10 \div 20$ nm followed by its hot pressing (see, for example, [7]). Taking into account these dimensions, nanograins can be treated as quantum wells and together with intergranular barriers and quantum structures containing barrier-well-barrier configurations can be considered. Thus, carrier tunneling through the barriers between nanoparticles and the quantum well becomes possible in such materials. Moreover, this model can account for possible resonant processes during the passage of a quantum nano-sized well and additional scattering of phonons at the boundaries of nanocrystals.

2. Model of quantum transport in nanostructured thermoelectric materials

Quantum transport in nanostructured thermoelectric materials, where the size of the nanograins is ranged of $10 \div 20$ nm, can be determined by two factors:

— the presence of an electric field with a potential difference $\Delta\varphi$, the magnitude of which for a nanograin under experimental conditions is $\Delta\varphi = (10^{-6} \div 10^{-4})$ V;
— the temperature gradient ΔT within the nanograin, where $\Delta T \sim 10^{-3}$ K.

Both of these factors can be interpreted as the presence of a certain potential field $e\Delta\varphi + k_0\Delta T$, where e is the electron charge and k_0 is the Boltzmann constant. For such a model, according to the Landauer quantum transport theory [8, 9], the tunneling current density through a nanograin, in the case where an external electric field $\Delta\varphi$ and a temperature gradient ΔT are applied, is given by the expression:

$$j = \frac{m^* e}{2\pi^2\hbar^3}\int_0^\infty \tau(E_x)\, I(E_x)\, dE_x, \tag{1}$$

where

$$I(E_x) = \int_{E_x}^{\infty} [f_0(E) - f_0(E - e\Delta\varphi - k_0\Delta T)]\, dE.$$

Let us note, that for the characteristic sample temperatures in the experiment, $T \sim 400\,\mathrm{K}$, the parameters

$$\alpha_1 = \frac{e\Delta\varphi}{k_0 T} \approx 0.01, \quad \alpha_2 = \frac{e\Delta E}{T} \approx 10^{-5}$$

are small, and therefore, when calculating $I(E_x)$ one can use the linearized approximation, with

$$I(E_x) = \int_{E_x}^{\infty} \frac{\partial f_0}{\partial E} \left(e\Delta\varphi + \frac{E-\mu}{k_0 T} \right) dE_\perp. \tag{2}$$

In this approximation, the heat flux density has the following form

$$j_q = \frac{m^* e}{2\pi^2\hbar^3} \int_0^{\infty} dE_x\, \tau(E_x) \int_{E_x}^{\infty} (E-\mu) \frac{\partial f_0}{\partial E} \left(e\Delta\varphi + \frac{E-\mu}{T}\Delta T \right) dE_\perp. \tag{3}$$

The formulas (1), (2), (3) allow us to obtain the well-known expressions for specific electrical conductivity [10],

$$\sigma = \sigma_0 \int_0^{\infty} \tau(E_x)\, f_0 \left(\frac{E_x - \mu}{k_0 T} \right) dE_x, \tag{4}$$

and the thermoelectric force coefficient

$$S = S_0 \frac{\int_0^{\infty} T(E_x) \left[\frac{E_x-\mu}{k_0 T} f_0\big(\frac{E_x-\mu}{k_0 T}\big) + \ln\Big(1 + \exp\big(-\frac{(E_x-\mu)}{k_0 T}\big)\Big) \right] dE_x}{\int_0^{\infty} T(E_x)\, f_0\big(\frac{E_x-\mu}{k_0 T}\big) dE_x}, \tag{5}$$

where $\sigma_0 = \frac{me^2 a E_0}{4\pi^2\hbar^3}$ and is approximately $2000\,\mathrm{Om}^{-1}\mathrm{m}^{-1}$ and $S_0 = \frac{k_0}{e}$ and is approximately $100\,\mu\mathrm{V/K}$.

The expressions (4) for σ and (5) for S can be subjected to numerical analysis in the case of a known transmission coefficient $\tau(E_x)$.

3. Calculation of $\tau(E)$

The transmission coefficient τ of a carrier through a nanodot can be calculated when the wave function ψ in the nanodot is known. We will model the nanodot with a quantum structure of the "barrier–well–barrier" type with potentials

$$V(x) = V_1(x) + V_2(x) + V_3(x), \tag{6}$$

where the components V_1, V_2, V_3 are Gaussian-type potentials

$$V_1 = V_0^{(1)} \exp\left(-\frac{(x-x_1)^2}{2w_1^2} \right), \quad V_2 = V_0^{(2)} \exp\left(-\frac{(x-x_2)^2}{2w_2^2} \right), \quad V_3 = V_0^{(3)} \exp\left(-\frac{(x-x_3)^2}{2w_3^2} \right). \tag{7}$$

The wave function ψ is the solution of the Schrödinger equation

$$-\frac{\hbar^2}{2m^*} \frac{d^2\psi}{dx^2} + V(x)\,\psi = E\psi, \tag{8}$$

where $V(x)$ is given by expression (6). For convenience, we model the potential energy $V(x)$ within the boundaries of the nanoisland by choosing the units for the parameters $V_0^{(i)}$, $(i = 1, 2, 3)$ and w_i, $(i = 1 \div 3)$ as $a_0 = 1\,\mathrm{nm}$, $E_0 = \frac{\hbar^2}{2m^* a_0^2}$. Thus,

$$V_0^{(1)} = V_0^{(3)} = E_0, \quad w_1 = w_3 = 1/3a_0, \quad V_0^{(2)} = E_0, \quad w_2 = a_0,$$
$$x_1 = a_0, \quad x_2 = 5a_0, \quad x_3 = 9a_0, \quad \varsigma = \frac{w}{a_0},$$
$$V(x) = E_0 \exp\big(-9a_0(x-1)^2\big) - E_0 \exp\big(-a_0(x-5)^2\big) + E_0 \exp\big(-9a_0(x-9)^2\big).$$

Figure 1 schematically presents the potential $V(x)/E_0$ within a nanoisland of size $10\,a_0$ along the $0X$-axis.

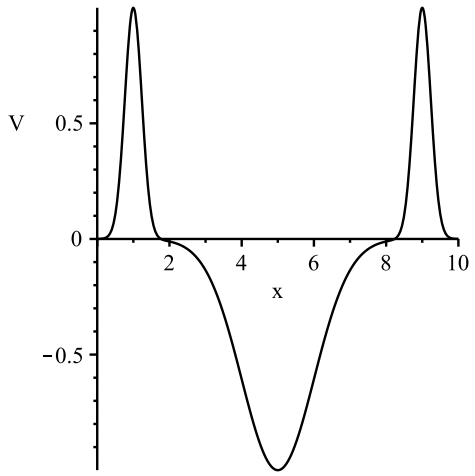

Fig. 1. The potential energy diagram of the nanograin for the Gaussian function parameters is as follows: $V_0 = 1$, the half-width of the barriers is $\varsigma = 1/3$, the half-width of the well is $\varsigma = 1$, and the depth of the well is equal to one relative unit.

For the model (7) of the potential $V(x)$ the Schrödinger equation allows a numerical solution only. We reformulate equation (8), using finite differences for a uniform grid on the interval $[0, 10]$. If Δ is the discretisation step and $n = 1 \div N - 1$, is the grid node index, then equation (8) is the following form

$$\frac{\psi_{n-1} - 2\psi_n + \psi_{n+1}}{\Delta^2} + \frac{2m}{\hbar^2}(E - V_n)\psi_n = 0,$$
$$n = 1, 2, \ldots, N - 1.$$

Alternatively, in dimensionless form the Schrödinger equation is presented as

$$\psi_{n-1} + u_n\psi_n + \psi_{n+1} = 0, \quad n = 1, 2, \ldots, N - 1, \qquad (9)$$

where $u_n = \varepsilon - v_n - 2$, $v_n = V_n/E_0$, $\varepsilon = E/E_0$, $n = 1 \div N - 1$. To solve the finite difference equations (9) we will apply the Thomas algorithm [11] along with the boundary conditions

$$\psi_1 + (0.5u_0 + i\,k\,\Delta)\psi_0 = 2i\,k\,\Delta,$$
$$\psi_{N-1} + (0.5u_n + i\,k\,\Delta)\psi_N = 0.$$

The solution to equation (9) will be found in the form of

$$\psi_{n+1} = R_n\psi_n$$

and we obtain the recurrence relation for R_n,

$$R_{n-1} = -\frac{1}{R_n + u_n}. \qquad (10)$$

From the boundary condition at the right end of the interval, One can find

$$R_{N-1} = -\frac{1}{0.5u_n + ik\Delta}, \qquad (11)$$

where the dimensionless wave number k is given by $k = \sqrt{E/E_0}$. If starting from the determined by the relation (11) R_{N-1}, using the recurrence relation (10), R_{N-2} can be found and so on, moving from the $(N-1)$th node to the node 0. By sequentially calculating R_{N-2}, R_{N-3}, …, R_1, R_0 we will find all N values of R_n, $(n = 0, 1, \ldots, N)$. Now, moving in the reverse direction from the node 0 to the $(N-1)$th node using (9), we will sequentially find the wave function at all internal nodes of the grid ψ_1, ψ_2, …, ψ_N. Knowing the wave function N-th node, we can calculate the transmission coefficient

$$\tau(E_x) = |\psi_N|^2.$$

Table 1. The dependence of the transmission coefficient of a particle through a barrier structure 'barrier–well–barrier' on its energy, calculated using the method Thomas algorithm.

ε	0.0	0.1	0.2	0.3	0.4	0.5	0.6	0.7	0.8	0.9
$\tau(\varepsilon)$	0.0	0.001	0.005	0.022	0.128	0.457	0.570	0.365	0.362	0.457
ε	1.0	1.1	1.2	1.3	1.4	1.5	1.6	1.7	1.8	1.9
$\tau(\varepsilon)$	0.646	0.881	0.999	0.939	0.825	0.741	0.701	0.699	0.726	0.775
ε	2.0	2.1	2.2	2.3	2.4	2.5	2.6	2.7	2.8	2.9
$\tau(\varepsilon)$	0.837	0.899	0.952	0.985	0.999	0.997	0.986	0.972	0.961	0.952
ε	3.0	3.1	3.2	3.3	3.4	3.5	3.6	3.7	3.8	3.9
$\tau(\varepsilon)$	0.951	0.956	0.963	0.971	0.979	0.987	0.992	0.997	0.999	1.0

Table 1 presents the results of calculations $\tau(E_x)$ for different incident particle energies in the range from zero energy to four relative units. Outside this range, $\tau(E_x)$ takes values equal to one relative unit.

4. The results of numerical modeling of the electrical conductivity σ and the Seebeck coefficient S

The obtained array for $\tau(E_x)$ makes possible the numerical calculation of the electrical conductivity σ and the Seebeck coefficient S, using expressions (4) and (5). A study was conducted on the temperature dependencies of the electrical conductivity σ, the Seebeck coefficient S, and the power factor $\sigma \cdot S^2$ based on the height of intergranular barriers, their width, and the distance between them, i.e., the size of the nanograins.

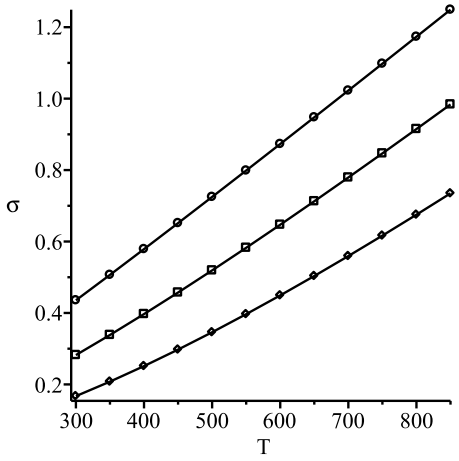

Fig. 2. The temperature dependence of the electrical conductivity as a function of the barrier height V_0: "○" — for $V_0 = 1$, "□" — for $V_0 = 1.5$, "◊" — for $V_0 = 2$.

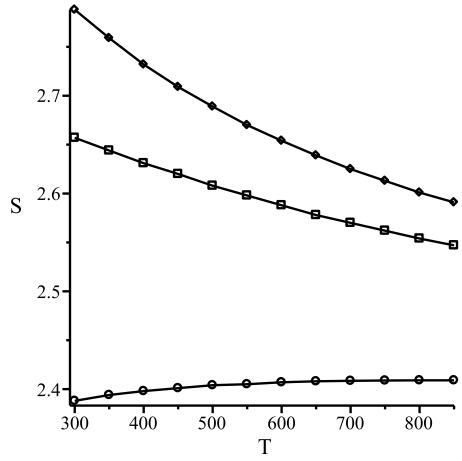

Fig. 3. The temperature dependence of the Seebeck coefficient on the barrier height V_0: "○" — for $V_0 = 1$, "□" — for $V_0 = 1.5$, "◊" — for $V_0 = 2$.

As seen from the graphs in Figure 2, with an increase in barrier height, the electrical conductivity significantly decreases. Specifically, when the barrier height doubles, the decrease in electrical conductivity is also close to a factor of two.

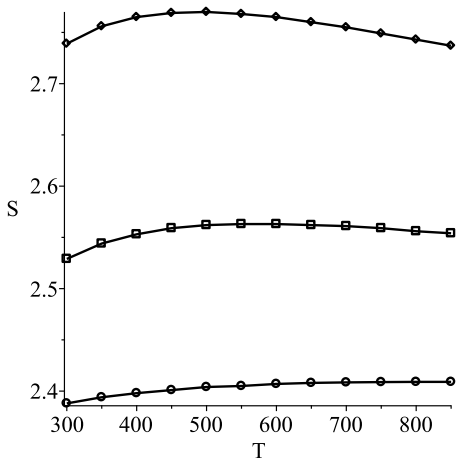

Fig. 4. The temperature dependence of the Seebeck coefficient on the barrier width: "○" — for half weight $\varsigma = 1/3$, "□" — for half weight $\varsigma = 0.5$, "◊" — for half weight $\varsigma = 1/\sqrt{2}$.

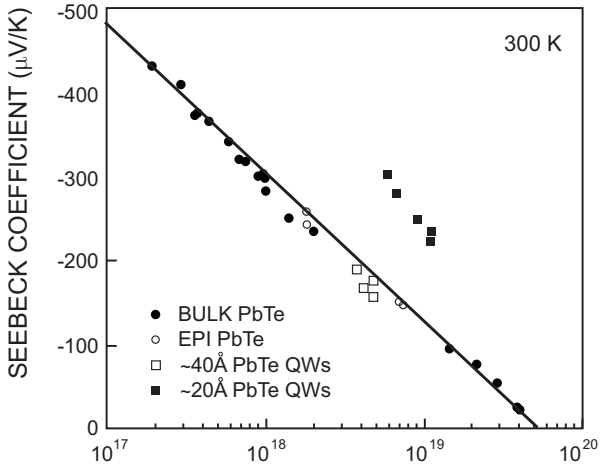

Fig. 5. Experimental results for the Seebeck coefficient for the material with quantum wells are presented in [4].

A similar behaviour is observed in the dependence of electrical conductivity on the barrier width. From the graphs presented in Figures 3 and 4 it is evident, that when the height of the barrier is doubled, and by approximately the same half-width i.e. from about ~ 0.3 to ~ 0.7 the Seebeck coefficient increases by approximately 20 percents.

It is interesting to note, as seen in Figure 5, that with an increase in barrier height, the power factor slightly increases. Specifically, when the barrier height triples, its increase does not exceed 40 percents.

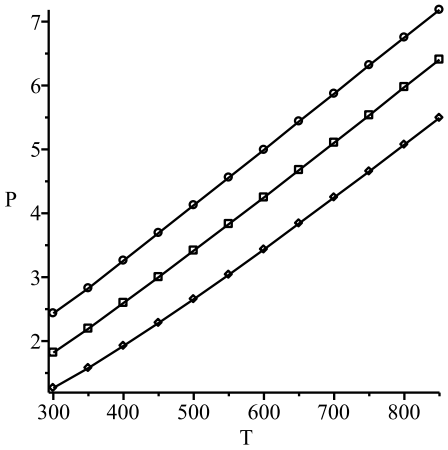

Fig. 6. The power factor, defined in relative units as $P = \frac{\sigma S^2}{\sigma_0 S_0^2}$, is presented as a function of temperature with a barrier distance of $b = 6$. The following symbols represent different barrier heights V_0: "○" for $V_0 = 3$, "□" for $V_0 = 2$, and "◇" for $V_0 = 1$.

For comparison, we present a graph of experimentally obtained results for the Pb Te/Pb Eu Te material with quantum wells. Figure 6 displays the Seebeck coefficient at a temperature of 300 K as a function of carrier concentration. It is noteworthy, that the measurements reflected the contribution to the thermoelectric effect from the tunneling mechanism and the contribution from the crystal lattice. However, the magnitude and the nature of the dependency of the studied parameter are consistent with the results obtained in our research.

At the same time, changes in the distance between barriers, i.e., the width of the well, have a minor influence on the thermoelectric characteristics of the proposed quantum structure. This means, that the presence of resonant tunneling minimally affects as the Seebeck coefficient and the power factor of the nanostructured material as well.

It should be noted, that the obtained values of the thermoelectric characteristics and their behaviour with changes in temperature and quantum structure parameters are consistent with the results, obtained by other authors, including [5, 10, 12, 13].

5. Conclusions

A one-dimensional model of a nanostructured thermoelectric material is studied, where the nanograin is modeled as a potential well, and the intergrain boundaries are represented by potential barriers. The well and barriers are modeled, using a Gaussian potential with te various parameters.

The modeling process was implemented as a program developed on the Maple computational mathematics platform. Using this program, the temperature dependencies of the electrical conductivity σ, the Seebeck coefficient S, and the power factor σS^2 were calculated and graphically illustrated.

It was shown, that as the height and width of the barriers increase, the conductivity of the quantum structure decreases, while the Seebeck coefficient increases. At the same time, the power factor σS^2 decreases with increasing barrier height, and changes in the distance between the barriers, i.e., the width of the well, have minor effect on the thermoelectric characteristics of the proposed quantum structure.

Appendix. Derivation of the expression for specific conductivity

Using the expression for the density of the tunneling current

$$j = \frac{m^* e}{2\pi^2\hbar^3}\int_0^\infty dE_x\,\tau(E_x)\int_{E_x}^\infty \left[f_0(E) - f_0(E - e\Delta\varphi - k_0\Delta T)\right] dE,$$

and considering that

$$f_0\left(\frac{E-(\mu+e\Delta V)}{k_0T}\right) \approx f_0(E) - \frac{\partial f_0(E)}{\partial E}e\Delta V + \frac{\partial f_0(E)}{\partial T}\Delta T.$$

We arrive at the following expression for the current density

$$j = \frac{me}{2\pi^2\hbar^3}\int_0^\infty dE_x\,T(E_x)\int_{E_x}^\infty \frac{\partial f_0(E)}{\partial E}\left(e\Delta V + \frac{E-\mu}{T}\Delta T\right) dE.$$

Here, E_x is the kinetic energy of the carrier along the axis $0x$, while $E = E_x + E_\perp$ is the energy corresponding to all three degrees of motion.

Now, let us assume that there is no temperature gradient in the system. Then

$$j = \frac{me^2}{2\pi^2\hbar^3}\int_0^\infty dE_x\, T(E_x)\int_{E_x}^\infty \frac{\partial f_0(E)}{\partial E}\Delta V\, dE.$$

Considering that

$$\int_{E_x}^\infty \frac{\partial f_0(E-\mu)}{\partial E}\, dE = -f_0(E_x-\mu),$$

we obtain the expression for the current density

$$j = \frac{me^2}{2\pi^2\hbar^3}\int_0^\infty f_0(E_x-\mu)\, T(E_x)\, dE_x\, \Delta V.$$

Since the electric field intensity of the external field is defined as $\frac{\Delta V}{a}$, the expression for the specific electrical conductivity will be

$$\sigma = \frac{me^2 a}{2\pi^2\hbar^3}\int T(E_x)\, f_0(E_x-\mu)\, dE_x = \sigma_0 \int T(E_x)\, f_0(E_x-\mu)\, dE_x,$$

where

$$\sigma_0 = \frac{me^2 a E_0}{2\pi^2\hbar^3} \simeq 2000\,\mathrm{Om}^{-1}\mathrm{m}^{-1}.$$

In the latter expression, it is taken into account that in the integrand, quantities with energy dimensions are expressed in relative units, i.e. E/E_0.

[1] Hicks L. D., Dresselhaus M. S. Effect of quantum-well structures on the thermoelectric figure of merit. Physical Review B. **47** (19), 12727–12731 (1993).

[2] Hicks L. D., Harman T. C., Dresselhaus M. S. Use of quantum-well superlattices to obtain a high figure of merit fromnonconventional thermoelectric materials. Applied Physics Letters. **63** (23), 3230–3232 (1993).

[3] Hicks L. D., Harman T. C., Sun X., Dresselhaus M. S. Experimental study of the effect of quantum-well structures on the thermoelectric figure of merit. Physical Review B. **53** (16), R10493–R10496 (1996).

[4] Harman T. C., Spears D. L., Manfra M. J. High thermoelectric figures of merit in Pb Te quantum wells. Journal of Electronic Materials. **25** (7), 1121–1127 (1996).

[5] Dresselhaus M. S., Chen G., Tang M. Y., Yang R. G., Lee H., Wang D. Z., Ren Z. F., Fleurial J.-P., Gogna P. New directions for low-dimensional thermoelectric materials. Advanced Materials. **19** (8), 1043–1053 (2007).

[6] Venkatasubramanian R., Siivola E., Colpitts T., O'Quinn B. Thin-film thermoelectric devices with high room-temperature figures of merit. Nature. **413**, 597–602 (2001).

[7] Zide J. M. O., Vashaee D., Bian Z. X., Zeng G., Bowers J. E., Shakouri A., Gossard A. C. Demonstration of electron filtering to increase the Seebeck coefficient in $In_{0.53}Ga_{0.47}As/In_{0.53}Ga_{0.28}Al_{0.19}As$ superlattices. Physical Review B. **74** (20), 205335 (2006).

[8] Landauer R. Spatial variation of currents and fields due to localized scatterers in metallic conduction. IBM Journal of Research and Development. **1** (3), 223–231 (1957).

[9] Landauer R. Electrical resistance of disordered one dimensional lattices. Philosophical Magazine. **21** (172), 863–867 (1970).

[10] Pichanusakorn P., Bandaru P. Nanostructured thermoelectrics. Materials Science and Engineering: R: Reports. **67** (2–4), 19–63 (2010).

[11] Ahuja P. Introduction to Numerical Methods in Chemical Engineering. 1.1 Tridiagonal matrix algorithm (TDMA). PHI Learning Pvt. Ltd. (2010).

[12] Gomez S. S., Romero R. Few-electron semiconductor quantum dots with Gaussian confinement. Open Physics. **7** (1), 12–21 (2009).

[13] Sun Y., Liu Y., Li R., Li Y., Bai S. Strategies to improve the thermoelectric figure of merit in thermoelectric functional materials. Frontiers in Chemistry. **10**, 865281 (2022).

Моделювання термоелектричних характеристик наноструктурованого матеріалу

Возняк О. М.[1], Костробій П. П.[2], Польовий В. Є.[2]

[1]*Прикарпатський національний університет імені Василя Стефаника, вул. Шевченка, 57, 76018, м. Івано-Франківськ, Україна*
[2]*Національний університет "Львівська політехніка", вул. С. Бандери, 12, 79013, м. Львів, Україна*

Розглянуто одновимірну модель наноструктурованого термоелектричного матеріалу, в якій нанозерно моделюється потенціальною ямою, а міжзеренні межі — потенціальними бар'єрами. Яма і бар'єри моделюється потенціалами гауссівського типу. Розроблено програмний продукт для розрахунку коефіцієнту проходження через квантову структуру "бар'єр–яма–бар'єр", в основі якого закладено алгоритм Томаса. Проведені числові розрахунки питомої провідності та коефіцієнту термоерес для запропонованої моделі. Результати розрахунків добре узгоджуються із експериментальними даними.

Ключові слова: *квантово-тунельний механізм термоелектричних явищ; модель наноструктурованого матеріалу; коефіцієнт Зеебека; фактор потужності.*